Negative Stain Electron Microscopic Analysis Suggests O Antigen Expression in *Escherichia coli* strain K-12 May Prevent T4 Interactions with the Bacterial Surface

Naser (Milad) Biparva, Arya Ghazizadeh, Thomas Hoang, Sunny Sun

Department of Microbiology and Immunology, University of British Columbia, Vancouver, British Columbia, Canada

SUMMARY Expression of O16 antigen on the surface of *Escherichia coli* K-12 has been shown to confer resistance to bacteriophage T4-mediated lysis, however, the underlying mechanism of resistance is poorly understood. In this study, we investigated a potential bacteriophage resistance mechanism using the *Escherichia coli* K-12 substrains DFB1655 L9, which expresses the O16 antigen, along with the isogenic substrain MG1655 which does not. We hypothesize that O16 antigen expression may confer resistance by preventing T4 from accessing cell surface receptors, thereby inhibiting adsorption. We infected both MG1655 and DFB1655 L9 with T4 phage and fixed the cells for visualization by negative stain electron microscopy. We identified bacteriophage interacting with the outer membrane of MG1655, however, none were detected on DFB1655 L9. This finding suggests that O16 antigen may confer resistance by preventing bacteriophage T4 from interacting with the DFB1655 L9 cell surface. Furthermore, these results contribute to existing research on how O antigen serotypes can confer resistance to phage infection.

Published Online: 17 September 2019

Citation: Biparva NM, Ghazizadeh A, Hoang T, Sun S. 2019. Negative Stain Electron Microscopic Analysis Suggests O Antigen Expression in *Escherichia coli* strain K-12 May Prevent T4 Interactions with the Bacterial Surface. UJEMI 24:1-11

Editor: Julia Huggins, University of British Columbia

Address correspondence to: https://jemi.microbiology.ubc.ca/

INTRODUCTION

The outer membrane of gram-negative bacteria is composed of an asymmetric lipid bilayer: an inner leaflet of phospholipids and an outer leaflet containing lipopolysaccharide (LPS) (1). LPS is comprised of an innermost lipid A section which is covalently linked to a polysaccharide core and occasionally sugar moieties known as O antigen (1). O antigen is comprised of repeating sets of glycan polymers of 2 to 8 sugar residues (2, 3). Variations in sugars, polymer linkages, and sugar arrangements result in a diverse array of O antigens (3,4). O antigen comprises the outermost portion of the LPS and interacts directly with the cell surface (1). In addition to LPS, the outer membrane contains receptors such as outer membrane proteins which can be sites of bacteriophage adsorption. While some bacteriophages use O antigen as a viral receptor, O antigens can also confer protection against other viruses, such as O16 antigen and bacteriophage T4 (5,6).

The bacteriophage T4 contains a 169 kb double-stranded DNA genome packaged into hemi-icosahedral head that is attached to a cylindrical tail with short and long tail fibers (7). Similar to other bacteriophages, direct binding of T4 tail fibers to exposed bacterial receptors is required in order for the bacteriophage T4 to bind and enter the cell (8). T4 receptors differ between bacterial strains. In the case of *E. coli* K-12, the outer membrane protein OmpC and the lipid A core region of LPS serve as receptors for T4 adsorption (9). Specifically, T4 long tail fibers bind reversibly to LPS glucose residues and OmpC (10). This is followed by irreversible binding of short tail fibers with the LPS core structure (10,11). The T4 tail then punctures the envelope, injecting the viral genome into the *E. coli* cytoplasm (11). This is followed by viral replication and ultimately cell lysis after approximately 25 minutes, releasing infectious viral progeny (12). Remarkably, expression of O16 antigen in K-12 substrain DFB1655 L9 results in T4 resistance, as well as resistance to bacteriophages T7 and P1 (5,6,13,14). However, the isogenic MG1655 substrain lacking O16 antigen is susceptible.

T4 resistance mediated by O antigen has been shown through growth curve analysis comparing MG1655 and DFB1655 L9. MG1655 infected with T4 displayed no growth by 210 minutes with no change in optical density (a measurement of cell lysis). By comparison, DFB1655 L9 displayed an observable increase in optical density in the same

timeframe (14). Resistance of DFB1655 L9 against bacteriophage T4 infection has also been observed in double overlay plaque assays compared to MG1655. MG1655 inoculated with T4 formed plaques at all viral dilutions, whereas DFB1655 L9 did not form plaques at any dilutions (5,13,14). These studies suggest that DFB1655 L9 is completely resistant to T4 bacteriophage infection (5,13,14). To elucidate the resistance mechanism, two separate studies performed qPCR assays to measure unadsorbed T4 titres after infection of MG1655 and DFB1655 L9 cells (13,14). Using qPCR targeting the T4-specific *gp23* gene, Wachtel *et al.* observed that at a multiplicity of infection (MOI) of 10^{-3} (1000 bacterial cells per virus), an average of $4.9x10^6$ more copies of *gp23* were detected in the unadsorbed fraction of DFB1655 L9 compared to MG1655 (13). This observation suggests that O16 antigen on DFB1655 L9 may decrease the interaction between the T4 phage and the bacterial outer membrane (13). On the other hand, a similar qPCR assay repeated by Lee *et al.* showed no significant differences in supernatant *gp23* copy number between MG1655 and DFB1655 L9 infected cells (14). Lee *et al.* suggest that while O16 confers resistance against bacteriophage T4, it does not prevent T4 binding to *E. coli* cells (14). Since the studies performed by Lee *et al*. and Wachtel *et al*. show conflicting results, we chose to investigate the mechanism of DFB1655 L9 resistance to bacteriophage T4 further (13, 14).

In this study, we visualized *E. coli* K-12 substrains DFB1655 L9 and MG1655 incubated with bacteriophage T4 using negative stain electron microscopy. We hypothesized that the presence of O16 antigen in substrain DFB1655 L9 could perturb interactions between the virus and the cell surface, which could account for the observed resistance phenotype (9,10).

METHODS AND MATERIALS

***E. coli* strains.** *E. coli* K-12 substrains MG1655 and DFB1655 L9 were previously used in our laboratory. Both were originally obtained from Douglas F. Browning at the Henderson Laboratory at University of Birmingham (6). MG1655 is a genetically characterized strain of *E. coli* K-12 unable to synthesize O16 antigen due to an IS5 insertion in the *wbbL* gene, encoding a rhamnosyltransferase, of the *rfb* locus (6). DFB1655 L9 is derived from MG1655 by complementation and insertion of the functional *wbbL* gene into its chromosome, restoring its ability to synthesize O16 antigen (6). Bacteriophage T4 was previously propagated in the lab, and was originally obtained from Carolina Biological Supply (cat no. 12-4330). *E. coli* substrain MG1655 was grown on a 1.5% LB agar plate. *E. coli* substrain DFB1655 L9 was grown on a 1.5% LB agar plate supplemented with 50 ug/mL of kanamycin. Both plates were incubated overnight at 37°C. Isolated colonies obtained were streaked onto fresh media and used for later experiments as the working stocks.

PCR to confirm substrains. Overnight cultures of *E. coli* substrain MG1655 and DFB1655 L9 were prepared in 5 mL of liquid LB media. Genomic DNA was isolated following the manufacturer's protocol from the PureLink™ Genomic DNA Mini Kit (cat no. K18020-01). The purity and concentration of DNA were assessed using a NanoDrop 2000c spectrophotometer by Thermo Scientific. PCR was performed with isolated genomic DNA using Platinum Taq DNA polymerase from Invitrogen, according to manufacturer's protocol (Table 1). Primers specific to the *wbbL* gene were designed by Browning *et al.*, and previously used in the lab by Chiu *et al.* (5,6). PCR protocols were adapted from Wachtel *et*

Table 1. Primers specific to *E. coli* K-12 strain MG1655 *wbbL* gene. F and R represent forward and reverse primers.

Gene	Sequence (5' - 3')	GC Content	Tm	Size (bp)
wbbL	F:CCCGAATTCATATGGTATATATAATAATCGTTTCCC	33%	57.1°C	1994 (MG1655)
	R:CCCAAGCTTCTCGAGTTACGGGTGAAAAACTGATGAAATTC	44%	66.4°C	799 (DFB1655 L9)

al. (13). Primers were used at a final concentration of 0.2 uM per reaction. Template genomic DNA was used at 155 ng per reaction. The Bio-Rad T100™ Thermal Cycler was set to 5 mins of initial denaturation at 95°C, and 30 cycles of 30 secs of denaturation at 95°C, 45 secs annealing at 55°C, and 2.5 mins extension at 72°C, and 5 mins final extension at 72°C. PCR products were run on a 1% agarose gel in 1x TAE buffer at 80V for 100 mins. The gel was visualized using SYBR™ DNA Gel Stain from Invitrogen using a ChemiDoc™ MP Imaging System from Bio-Rad.

Propagation of phage working stocks. An overnight culture of MG1655 was diluted 1:5 a in LB. 10 uL of the laboratory bacteriophage T4 stock was added to the subculture and incubated by shaking overnight at 37°C. The next day, 300 uL of chloroform was added to the phage lysate, mixed by vortexing, and left to settle overnight at 4°C. The following day, the debris-free top fraction was collected and filter-sterilized using a 0.45 um syringe filter to create a working lysate.

PCR to confirm phage identity. PCR was performed with phage stock using Platinum Taq DNA polymerase from Invitrogen, according to manufacturer's protocol (Table 1). Primers used were specific to the *gp23* gene encoding a major capsid protein in bacteriophage T4 (5). PCR and gel electrophoresis were performed as described above; 2 uL of phage stock, and an annealing temperature of 51.3°C were used for this reaction and products were ran on a 1% agarose gel at 100V for 30 mins.

Double agar overlay plaque assay to enumerate bacteriophage T4 titre and confirm differential T4 susceptibility of substrains. Reagent preparation and methods were based on Wachtel *et al*. (13). LB media for the underlay plates was prepared at an agar density of 15 g/L and supplemented with sterile $CaCl_2$ to a final concentration of 0.5 mM. Once cooled, it was poured into Petri dishes and stored inverted at 4°C. LB media for the overlay was prepared at an agar density of 4g/L and supplemented with 0.5 mM of sterile $CaCl_2$, followed by storage at room temperature. 5 mL overnight cultures of MG1655 and DFB1655 L9 were prepared in LB broth. Before the experiment, the underlay plates were warmed in the 37°C incubator for 1 hour to remove condensation. The overlay agar was liquified in the microwave prior to the experiment, aliquoted into 50 mL working solutions, and kept in a 55°C water bath for the duration of the experiment. The purified phage lysate was serially diluted in LB from 10^{-1} to 10^{-9}. In a sterile glass tube, 2 mL of liquid overlay agar at 55°C, 100 uL of phage dilution, and 100 uL of either MG1655 or DFB1655 L9 was added. The solution was mixed immediately and poured onto an underlay plate. The plate was swirled to evenly to spread the liquid mixture consistently throughout the entire surface area before solidification. The plates were incubated overnight at 37°C, and the plaque forming units (PFUs) were counted the following day. The 10^{-6} dilution of phage plated with MG1655 showed countable number of plaques and the titre of bacteriophage T4 stock was calculated to be 1.00×10^9 PFU/mL.

Bacteriophage T4 and *E. coli* adsorption assay. 5 mL overnight cultures of MG1655 and DFB1655 L9 were prepared by inoculation from plates, and their OD_{600} was measured using the Pharmacia Biotech Ultrospec 3000 at 600 nm. The higher OD_{600} of the two substrains was diluted with LB to normalize to the lower OD_{600} determined to be 0.8 units. 500 uL of lab stock phage at 1.79×10^{10} PFU/mL was added to 500 uL of OD_{600}-normalized MG1655 or DFB1655 L9. Each sample was done in duplicate. The cells were infected for 5

Table 2. Primers specific to bacteriophage T4 *gp23* gene. F and R represent forward and reverse primers.

Gene	Sequence (5' - 3')	GC Content	Tm	Size (bp)
gp23	F:GCCATTACTGGAAGGTGAAGG	52%	54°C	398
	R:TTGGGTGGAATGCTTCTTTAG	43%	53°C	

min at 37°C to allow for adsorption but not viral replication (12,13). Afterwards, the samples were immediate centrifuged at 16,000 g for 2.5 mins at 4°C.

Negative stain electron microscopy. The adsorption assay supernatant was quickly removed and the cell pellets were fixed immediately for 15 minutes using a mixture of 4% formaldehyde (Electron Microscopy Sciences cat no. 15710) and 2.5% glutaraldehyde (TED PELLA, INC cat no. 492477) in a 1X PBS final concentration to terminate the infection. The mixture was pelleted at 16,000 g for 2.5 mins at 4°C and the fixative was discarded. The cells were washed 3 times by pelleting and resuspending in 1X PBS. After the last wash, the cells were suspended in 300 uL of 1X PBS. With assistance from technicians at the UBC Bioimaging Facility, 3 uL of the cell suspension was mounted on a glow-discharged electron microscopy grid, and after 30 secs, wicked off with filter paper. The grid was then stained with 5 uL of uranyl acetate (4% aqueous solution) for 30 secs and wicked off with filter paper. The samples were visualized under the Hitachi H7600 transmission electron microscope running at 80kV accelerating voltage with an AMT XR50 digital camera.

RESULTS

PCR analysis of *E. coli* K-12 MG1655 and *E. coli* DFB1655 L9. To confirm the identity of substrain MG1655 and DFB1655 L9, we performed PCR analysis using primers flanking the 799 bp *wbbL* gene (5). As expected from the gel electrophoresis, MG1655 showed a single band at 2.0 kbp which corresponds to the non-functional *wbbL* gene containing the 1.2 kbp IS5 insertion mutation (6). DFB1655 L9 shows a band at 800 bp and 2.0 kbp (Figure 1). The 800 bp band from the DFB1655 L9 PCR product corresponds to the expected 799 bp functional *wbbL* gene. The 2.0 kbp band from the DFB1655 L9 PCR product is due to the single crossover event of the *wbbL* gene, resulting in DFB1655 L9

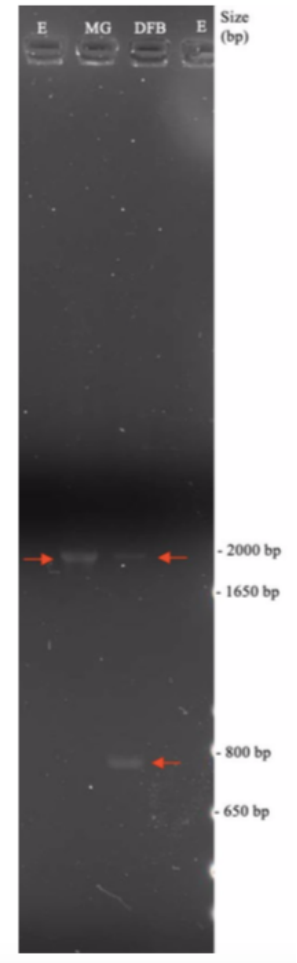

FIG. 1 PCR of the *wbbL* gene in *E. coli* K-12 substrains MG1655 and DFB1655 L9 indicates an intact *wbbL* gene in only DFB1655 L9. PCR was performed on the two substrains and the products were resolved on a 1.0% agarose gel. As expected, an intact *wbbL* gene of approximately 800 bp corresponding to functional O16 antigen biosynthesis is present only in the DFB1655 L9 substrain. Both substrains contain the 2.0 kbp amplicon corresponding to the non-functional *wbbL* gene containing the 1.2 kbp IS5 insertion mutation. E = Empty; DFB = DFB1655 L9 DNA; MG = MG1655 DNA.

chromosome containing both functional and non-functional *wbbL* genes (6). Our gel electrophoresis results are consistent with previous studies (5,13,14). Additionally, the faint bands could be due to excessive genomic template for PCR or non-specific PCR products. These PCR results confirm the expected *wbbL* genotypes of MG1655 and DFB1655 L9 (5,13,14).

PCR characterization of T4 bacteriophage. To confirm the identity of T4 bacteriophage in our laboratory stock and working lysate solutions, we used primer pairs targeting the *gp23* gene found in bacteriophage T4. For our laboratory stock and working lysates, the PCR results show a distinct band at approximately 400 bp (Figure 2). This corresponds to our expected *gp23* gene size present in bacteriophage T4 (15). The dH_2O negative control reactions showed no bands indicating the absence primer dimers or non-specific PCR products from contaminating DNA. These PCR results confirm the identity of bacteriophage T4 in our laboratory stock and working lysates.

***E. coli* K-12 substrain DFB1655 L9 is resistant to bacteriophage T4 infection.** To confirm the susceptibility of MG1655 and resistance of DFB1655 L9 to bacteriophage T4 infection, we performed a double overlay plaque assay. Serial dilutions of T4 phage lysates were plated on 0.5 mM $CaCl_2$ LB agar plates with either MG1655 or DFB1655 L9 and incubated overnight. Susceptibility to bacteriophage T4 was measured by plaque enumeration on the plate the next day (Figure 3). All MG1655 plates showed a concentration-dependent formation of plaques, countable at the 10^{-6} dilution. Plaques were uniform and approximately 2-3 mm in diameter, corresponding to the expected T4 plaque size (13, 14). The 10^{-6} dilution technical replicates resulted in 98 and 102 plaques, which were then used to calculate a 1.00 x 10^9 PFU/mL viral titre in our working lysates. As seen in Figure 3, DFB1655 L9 plates were devoid of plaques and grew confluent lawns,

FIG. 2 PCR of the *gp23* gene confirms identity of bacteriophage T4. PCR was performed on the stock and lysate solutions and products were imaged on a 1.0% agarose gel using reverse contrast. Bands of approximately 400 bp in the T4 stock and lysate solutions (1/5 and 1/50) indicate the presence of T4. T4 NC = Negative Control with T4 primers; T4 1/50 = Lysate from 1/50 bacterial solution; T4 1/5 = Lysate from 1/5 bacterial solution; T4 Stock = Lysate from initial stock.

regardless of the plated phage dilution. As a negative control, LB without T4 bacteriophage was added to MG1655 and DFB1655 L9 samples. Both negative control conditions grew as confluent lawns and showed no plaques (data not shown). Taken together, these results align with previous studies reporting susceptibility to bacteriophage T4-mediated lysis in MG1655 but not DFB1655 L9 (5,13,14).

Negative stain electron microscopy shows bacteriophage T4 on the surface of MG1655 but not DFB1655 L9. To visualize the interaction of bacteriophage T4 with MG1655 and DFB1655 L9, we performed negative stain electron microscopy. Using overnight cultures of MG1655 and DFB1655 L9, we infected each substrain with lab stock phage at a concentration of 1.79 x 10^{10} PFU/mL. After 5 minutes, we pelleted the bacterial cells by centrifugation. The cells were immediately fixed and subsequently processed for negative stain electron microscopy. We observed bacteriophage T4 attached to the outer membrane

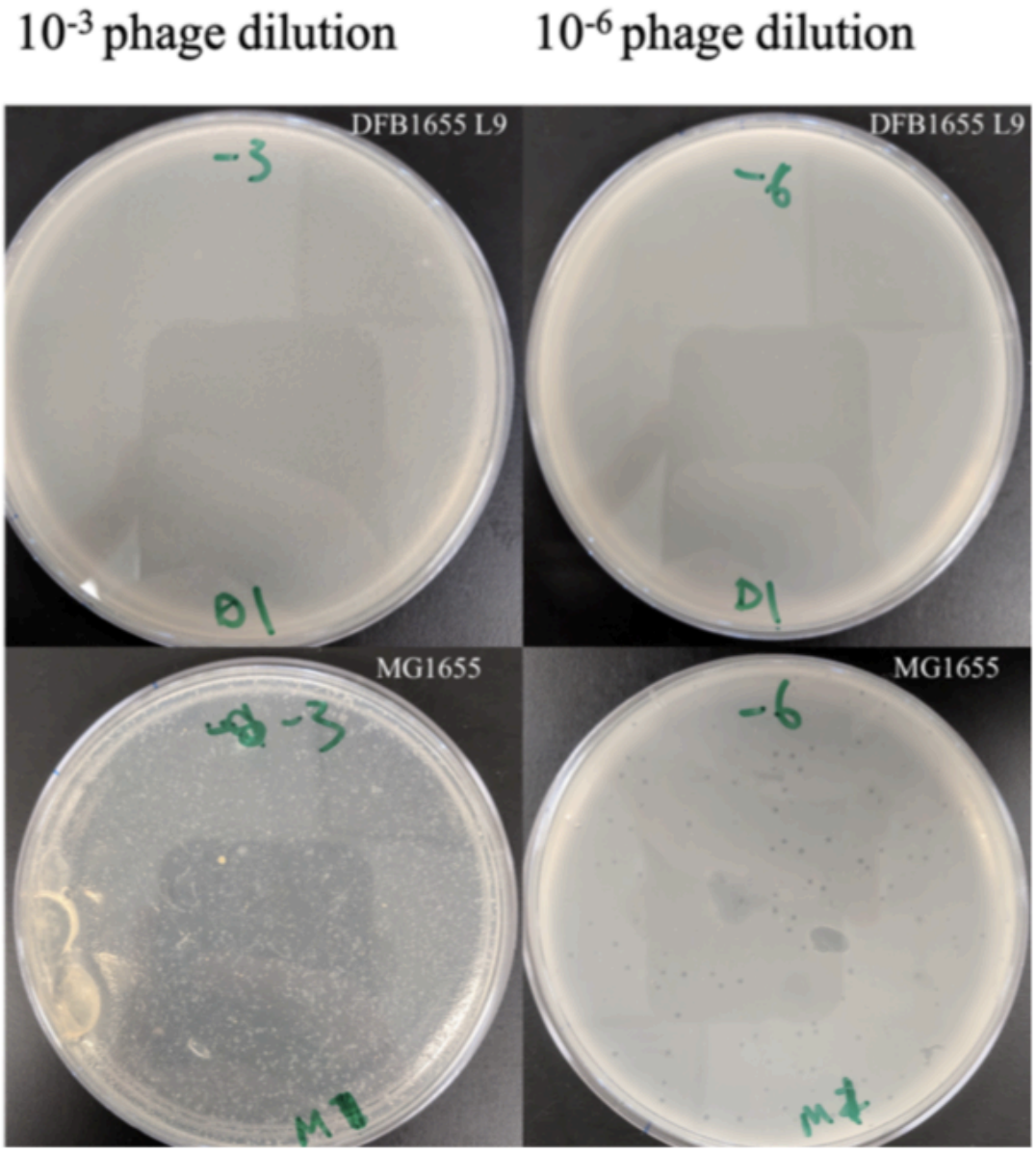

FIG. 3 DFB1655 L9 displays no plaque formation compared to MG1655, confirming the resistance of DFB1655 L9 to bacteriophage T4 infection. Shown are representative images of the concentration-dependent lysis of MG1655 due to bacteriophage T4 infection. Images on the left contain a higher plated bacteriophage T4 titre compared to images on the right. All titres show no plaque formation for DFB1655 L9. LB plates containing 0.5 mM $CaCl_2$ were incubated at 37°C.

of MG1655 (Figure 4). The appearance of T4 is consistent with previous literature as they are approximately 90 nm wide, 200 nm long with a hemi-icosahedral capsid (Figure 4) (7,16,17). The capsids, tails, and fibers are clearly distinguishable. Additionally, phage tail fibers appear to be embedded in the outer membrane while the viral capsids remain visible and associated with the bacterial surface, consistent with viral adsorption (8,17). Further, some phages appear tipped over (Figure 4). The phage in Figure 4f appears to have one of its fibers embedded in the membrane, while the other fibers are detached from the bacteria, possibly in the process of binding to the membrane (Figure 4). In contrast, DFB1655 L9 samples show no interaction with bacteriophage T4 as we could not locate any bacteriophage T4 on DFB1655 L9 in any field of view (Figure 5). As for the substrains themselves, MG1655 and DFB1655 L9 both display general morphology consistent with *E. coli* K-12. Namely, they are predominantly rod-shaped and are approximately 1 micron wide, however there are some notable differences between the two (Figures 4 and 5) (6). DFB1655 L9 appears to be more elongated compared to MG1655 and also show darker staining, possibly due to greater stain uptake in the presence of O16 antigen (Figures 4 and 5). This elongated cell shape for DFB1655 L9 was also observed in two previous independent experiments and the difference between the two substrains could be the subject of future study (data not shown). We were unable to normalize the number of attached phages to the total number of bacteria per electron microscopy grid due to time constraints and the qualitative nature of this method.

The observation of phages on the surface of MG1655 and not DFB1655 L9 aligns with our initial hypothesis suggesting that O16 antigen confers resistance to bacteriophage T4 infection by preventing interactions between the phage and the bacterial surface.

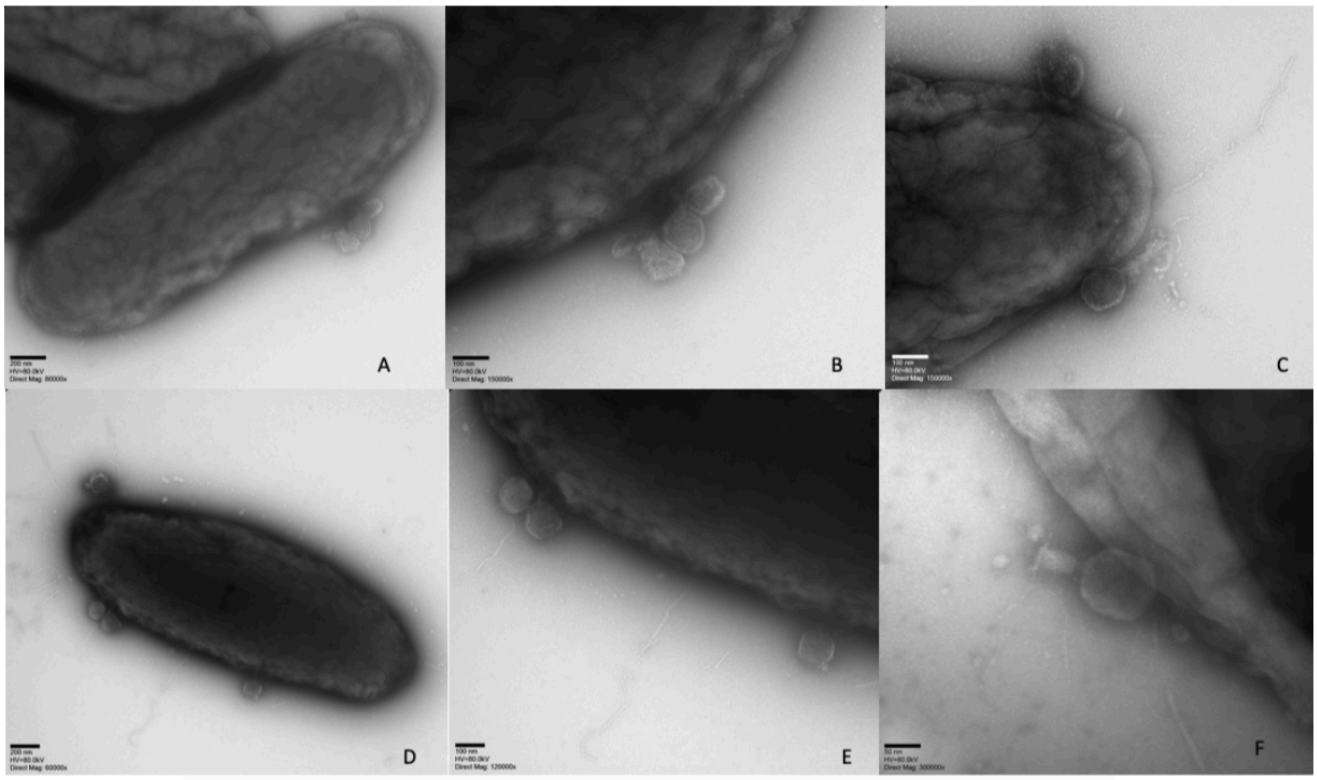

FIG. 4 Negative stain electron microscopy shows T4 interacting with MG1655. The MG1655 samples were infected with T4 for 5 minutes, and were subsequently prepared for visualization under electron microscopy. The images above display T4 phages attached to the cell membrane of MG1655 during the first 5 minutes of infection. (B) and (E) are magnified versions of (A) and (D) respectively, to more clearly visualize the capsid ultrastructure. The phages are approximately 90 nm in width and 200 nm in length, and their capsids, tails, and long tail fibers are distinguishable in some of the above images. MG1655 shows the long, rod shaped characteristic of *E. coli* K-12. In (F), 1 = long tail fibers, 2 = tail, 3 = capsid. Direct magnifications and scale bars for images are as follows: A = 80,000x, 200 nm; B = 150,000x, 100 nm; C = 150,000x, 100 nm; D = 60,000x, 200 nm; E = 120,000x, 100 nm; F = 300,000x, 50 nm.

DISCUSSION

Bacteriophage research has shown a resurgence in the fields of microbial ecology and medicine (19). Given the critical role of bacteriophage in dissolved organic material turnover and the potential for combating antimicrobial resistance, further research is required to better understand interactions between phage and bacteria (19, 20). Our study investigated resistance of *E. coli* K-12 substrain DFB1655 L9 to bacteriophage T4 infection (5, 13, 14). DFB1655 L9 is a strain engineered to express O antigen, made possible by genomic insertion of a functional *wbbL* rhamnosyltransferase gene into MG1655 (6). DFB1655 L9 is also resistant to bacteriophage T7 of the *Podoviridae* family, and bacteriophage P1 of the *Myoviridae* family. Taken together, these observations suggest O16 antigen confers resistance to multiple bacteriophages, however the underlying mechanism is not well understood. Insertion of the *wbbL* gene results in expression of O16 antigen, a glycan polymer tethered to the LPS outer core. Thus, it is conceivable that steric hindrance mediated by surface-expressed O antigen could inhibit T4 interactions with the bacterial cell surface (6). Our data appears to align with the results of Wachtel *et al*. who observed higher levels of DFB1655 L9 in culture supernatants compared to MG1655. Thus, our results are inconsistent with Lee *et al.* who indicated adsorption may not explain the resistance phenotype after observing no difference in *gp23* copy number in the supernatants of T4-infected DFB1655 L9 or MG1655.

Initially, our study sought to repeat the adsorption assays described in Wachtel *et al.* and Lee *et al.*, and quantify unadsorbed virus using a plaque assay. However, we were unable to detect differences in the number of unadsorbed viable viruses, likely due to technical reasons – we used a low number of bacteria as an adsorption substrate. Thus, we decided to use negative stain electron microscopy to directly image adsorbed phages, a

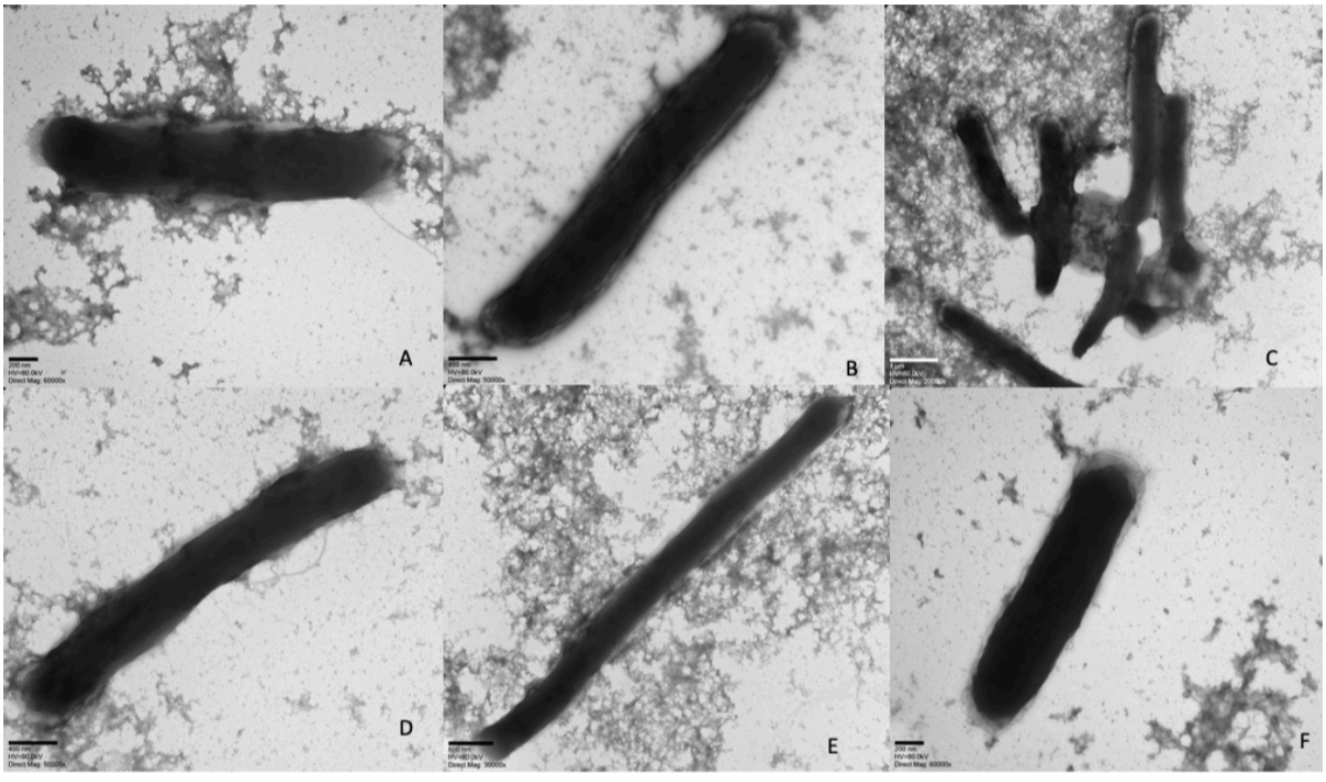

FIG. 5 Negative stain electron microscopy of DFB1655 L9 samples reveal no attached T4. The DFB1655 L9 samples were infected with T4 for 5 minutes, and were subsequently prepared for visualization under electron microscopy. The images above display DFB1655 L9 devoid of any attached T4 phages, and are representative of all fields of view. DFB1655 L9 displays varying lengths and sizes, but shows the consistent long, rod shaped characteristics of *E. coli* cells. The amorphous background structures are crosslinked LB proteins which were not successfully washed from the samples during preparation for negative staining electron microscopy. Direct magnifications and scale bars for images are as follows: A = 60,000x, 200 nm; B = 50,000x, 400 nm; C = 20,000x , 1 um; D = 50,000x, 400 nm; E = 30,000x, 600 nm; F = 60,000x, 200 nm.

more direct approach to visualize qualitative differences in viral adsorption. Negative stain electron microscopy is a simple and inexpensive technique that permits rapid visualization of phage-bacterium interactions. We were unable to detect virus attached to DFB1655 L9 in any orientation across the entire EM field of view. Conversely, MG1655 displayed many phage attachments, including single cells with numerous phages attached despite identical cell number and MOI. However, it is important to note that only ~10% of MG1655 had phage attached, although we could not quantify the number of MG1655 without phage attachments due to time constraints. Further, many phages were imaged in a binding orientation consistent with viral adsorption on the MG1655 cell surface: with tail spikes embedded into outer membrane and capsids visible above the cell surface. This result supports the hypothesis that O16 antigen prevents bacteriophage T4 interaction with the cell surface, thus corroborating the results of Wachtel *et al.* The total absence of phages on the surface of DFB1655 L9 suggests that O16 expression may prevent T4 interactions with the cell surface. This is consistent with the observation that DFB1655 L9 is resistant to T4 infection, displaying no plaques even when infected with phage titres as high as 10^{10} PFU/mL (13). It is important to note that our DFB1655 L9 samples, although prepared identically to MG1655, had more crosslinked proteins from the LB media in the background which could have prevented observation of phage. However, given the clear outline of the phage, and that it was also detected in zones with equally "dirty" backgrounds for MG1655, this should not have greatly impacted the observations. Furthermore, we used identical magnifications to initially detect virus for both MG1655 and DFB1655 L9 before concluding phage was present on the former but not latter. Thus, our electron micrographs for MG1655 focused mainly on the phage-bacterium interactions, while the DFB1655 L9 micrographs focused more on the bacterial ultrastructure as phage-bacterium interactions were not detected. While this results in different magnifications between Figures 4 and 5, it does not impact the observation itself.

In addition to imaging adsorbed phages, the use of negative stain electron microscopy also enabled us to visualize detailed structures of both MG1655 and DFB1655 L9. While Browning *et al.* showed both substrains have comparable growth kinetics and outer membrane composition (assessed by Western blotting and further staining for outer membrane structures using Hoechst and Propidium iodide stains) we noticed peculiar differences in cell shape and surface characteristics (6). First, we observed that the MG1655 surface had a "wrinkled" appearance, while the DFB1655 L9 had a "smoother" appearance. This characteristic could be explained by increased O antigen density in DFB1655 L9, leading to differential uptake of the stain. We also observed numerous filamentous DFB1655 L9 cells that were up to 20-fold longer than MG1655 cells, in this study as well as for two previous experiments (data not shown). Filamentation results from cell growth without septation and is a well-characterized bacterial cell stress response to DNA damage, heat, or inhibition of cell wall biosynthesis (21). Although this observation should be repeated, exploring how *wbbL* expression contributes to cell stress could be a potential avenue for further research.

Limitations A significant limitation of our study is that we only visualized phage-bacterium interactions once for both MG1655 and DFB1655 L9. This was due to lengthy optimization of the electron microscopy protocol, resulting in time constraints. In addition to our low sample size, we could not enumerate the number of phage-bearing bacteria per total bacteria in each grid. This prevented us from collecting quantitative data for statistical analyses in order to assess whether our observation was due to random chance.

Conclusions Our findings show that bacteriophage T4 interacts with the surface of substrain MG1655 but not DFB1655 L9. These results corroborate the hypothesis that resistance of DFB1655 to T4 infection may be due to the surface expression of O antigen which could perturb phage-bacterium interactions, leading to inhibition of viral attachment, and subsequently, adsorption.

.

Future Directions To further expand on this phenotype, future studies could investigate whether or not O16 antigen confers general resistance to numerous bacteriophages.

Previous studies have shown that DFB1655 L9 is resistant to bacteriophages P1, T4, and T7 (13, 14, 16). This suggests O16 antigen likely blocks viral attachment by sterically hindering viral access to the outer membrane. Thus, futures researchers could infect both MG1655 and DFB1655 L9 with numerous phages and screen for the presence of plaques. It could be possible MG1655 is resistant to certain phages, and that restoring O16 antigen biosynthesis results in phage susceptibility. This finding would show that O16 antigen could also be sufficient for susceptibility to certain phages. One major limitation of our findings was that we were unable to apply statistical analyses to our electron microscopy observations due to time constraints. Since it is possible our attachment phenotype was due to chance, future studies should count the number of bacteria bearing adsorbed phages and normalize this to the total number of bacteria per grid. This would further validate these observations by providing statistical support. Future studies could also examine whether the number of sugar moieties in O16 antigen is important in conferring resistance. This could be done by treating whole bacterial cells with various glycosyl hydrolases that truncate the O16 glycan polymer, followed by assessment of resistance. If enzymatic cleavage restores susceptibility, it is likely steric hindrance of viral attachment is the resistance mechanism. Finally, as mentioned above, a potentially exciting research direction would be to investigate further whether or not *wbbL* expression contributes to cell stress, resulting in the extensive filamentation we observed in DFB1655 L9 cells. Although this observation should be repeated first, performing RT-qPCR for stress response genes in both MG1655 and DFB1655 L9 would allow gene expression profiling of bacterial cell stress.

ACKNOWLEDGEMENTS

We would like to acknowledge Dr. Dave Oliver and Mihai Cirstea for their advice and technical guidance. We would also like to acknowledge Dr. Miki Fujita, Bradford Ross, and Derek Horne from the UBC Bioimaging Facility for assisting us with sample preparation and electron microscopy. Further, we would like to thank the Wesbrook Media Room Staff for providing us with glassware, and Dr. Douglas Browning from the University of Birmingham, UK, for providing the *E. coli* K-12 substrains MG1655 and DFB1655 L9 used in this study. Finally, we would like to thank the UBC Department of Microbiology & Immunology for funding this research.

REFERENCES

1. **Rakhuba, DV, Kolomiets, EI, Dey, ES, Novik, GI.** 2010. Bacteriophage receptors, mechanisms of phage adsorption and penetration into host cell. Pol J Microbiol. **59:**145.
2. 2. **Lerouge, I, Vanderleyden, J.** 2002. O-antigen structural variation: mechanisms and possible roles in animal/plant–microbe interactions. FEMS Microbiol Immunol. **26:**17-47. doi: 10.1111/j.1574-6976.2002.tb00597.x.
3. 3. **Wang, L, Wang, Q, Reeves, P.** 2010. The Variation of O Antigens in Gram-Negative Bacteria, p. 123-152. In Anonymous Endotoxins: Structure, Function and Recognition Vol. 53. Springer Netherlands, Dordrecht. doi: 10.1007/978-90-481-9078-2_6.
4. 4. **Raetz, CRH, Whitfield, C.** 2002. Lipopolysaccharide endotoxins. Annu Rev Biochem. **71:**635-700. doi: 10.1146/annurev.biochem.71.110601.135414.
5. 5. **Chiu, J, Croft, C, Ng, K.** 2017. *Escherichia coli* O antigen serotype O16 is a restriction factor for bacteriophage T4 infection. JEMI. **3:**38-44.
6. 6. **Browning, DF, Wells, TJ, França, FLS, Morris, FC, Sevastsyanovich, YR, Bryant, JA, Johnson, MD, Lund, PA, Cunningham, AF, Hobman, JL, May, RC, Webber, MA, Henderson, IR.** 2013. Laboratory adapted *Escherichia coli* K-12 becomes a pathogen of *Caenorhabditis elegans* upon restoration of O antigen biosynthesis. Mol Microbiol. **87:**939-950. doi: 10.1111/mmi.12144.
7. 7. **George P C Salmond, Peter C Fineran.** 2015. A century of the phage: past, present and future. Nat Rev Microbiol. **13:**777-786. doi: 10.1038/nrmicro3564.
8. 8. **Washizaki, A, Yonesaki, T, Otsuka, Y.** 2016. Characterization of the interactions between *Escherichia coli* receptors, LPS and OmpC, and bacteriophage T4 long tail fibers. Microbiologyopen. **5:**1003-1015. doi: 10.1002/mbo3.384.
9. 9. **F Yu, S Mizushima.** 1982. Roles of lipopolysaccharide and outer membrane protein OmpC of *Escherichia coli* K-12 in the receptor function for bacteriophage T4. J Bacteriol. **151:**718-722.
10. 10. **Ali, SA, Iwabuchi, N, Matsui, T, Hirota, K, Kidokoro, S, Arai, M, Kuwajima, K, Schuck, P, Arisaka, F.** 2003. Reversible and fast association equilibria of a molecular chaperone, *gp57A*, of bacteriophage T4. Biophys J. **85:**2606-2618. doi: 10.1016/S0006-3495(03)74683-9.

11. 11. **Kostyuchenko, VA, Mesyanzhinov, VV, Kanamaru, S, Arisaka, F, Leiman, PG, Rossmann, MG, Chipman, PR.** 2002. Structure of the cell-puncturing device of bacteriophage T4. Nature. **415:**553-557. doi: 10.1038/415553a.
12. 12. **S T Abedon.** 1992. Lysis of lysis-inhibited bacteriophage T4-infected cells. J Bacteriol. **174:**8073-8080. doi: 10.1128/jb.174.24.8073-8080.1992.
13. 13. **Wachtel, A, Guo, A, Sagorin, Z, Etti, E.** 2017. O16 Serotype O antigen expression in *Escherichia coli* K-12 may confer resistance against T4 bacteriophage infection by preventing adsorption. JEMI. **3:**70-79.
14. 14. **Lee, S, Bie, dB, Ngo, J, Lo, J.** 2018. O16 antigen confers resistance to bacteriophage T4 and T7 but does not reduce T4/T7 adsorption in *Escherichia coli* K-12. JEMI. **22:**1-11.
15. 15. **Heggen A, McLaughlin A, Russell G, Zhang A.** 2014. T4 bacteriophage may not inhibit transcription of T7 bacteriophage genes *rpol* and *gp10a* during co-infection of *Escherichia coli*. JEMI. **18**:162-166.
16. 16. **Ackermann H, Krisch H.** 1997. A catalogue of T4-type bacteriophages. Arch Virol. **142**:2329-2345. doi: 10.1007/s007050050246.
17. 17. **Yap M, Rossmann M.** 2014. Structure and function of bacteriophage T4. Future Microbiol. **9**:1319-1327. doi: 10.2217/fmb.14.91.
18. 18. **Andrew D. Millard, Martha R.J. Clokie, Andrey V. Letarov, Shaun Heaphy.** 2011. Phages in nature. Bacteriophage. **1:**31-45. doi: 10.4161/bact.1.1.14942.
19. 19. **Christine Miller, Line Elnif Thomsen, Carina Gaggero, Ronen Mosseri, Hanne Ingmer, Stanley N. Cohen.** 2004. SOS Response Induction by β-Lactams and Bacterial Defense against Antibiotic Lethality. Science. **305:**1629-1631.
20. 20. **Irshad Ul Haq, Waqas Nasir Chaudhry, Maha Nadeem Akhtar, Saadia Andleeb, Ishtiaq Qadri.** 2012. Bacteriophages and their implications on future biotechnology: a review. Virology Journal. **9:**9. doi: 10.1186/1743-422X-9-9.
21. 21. **Mavrich, TN, Hatfull, GF.** 2017. Bacteriophage evolution differs by host, lifestyle and genome. Nature Microbiology. **2:**17112. doi: 10.1038/nmicrobiol.2017.112.